REPLACING MULTI-LAYER PERCEPTRON WITH TAYLOR EXPANSION

Anonymous authors
Paper under double-blind review

ABSTRACT

The Multi-Layer Perceptron (MLP) constitutes a fundamental building block of deep learning. However, its inherent reliance on dense matrix multiplication imposes a substantial computational burden, especially on resource-constrained edge devices, which poses a critical challenge to the real-time inference requirements of edge artificial intelligence applications. In this paper, we propose T-MLP, a novel method that mitigates this challenge by approximating the MLP via a lightweight module that combines K-means and first-order Taylor expansion. Replaced by T-MLP, MLP online inference is reduced to a single K-means prediction, followed by one dense matrix multiplication and two element-wise additions. On a commercial edge device, T-MLP yields **$>$100×** speed-up on large-scale MLP with $< 1\%$ accuracy loss. Grounded in reduced time-complexity and hardware-friendly footprint, T-MLP establishes a new paradigm for edge-side efficient inference.

1 INTRODUCTION

The Multi-Layer Perceptron (MLP)(Popescu et al., 2009) is the foundational substrate of modern deep learning. An input layer, a output layer, and multiple hidden layers with nonlinear activation functions endow the MLP with rich representational power for complex classification and regression. With the rise of edge artificial intelligence, MLPs are ubiquitously deployed on edge devices across a diverse range of tasks, including image classification(Lin et al., 2020; 2021; Howard et al., 2017; Sandler et al., 2018), network intrusion detection(Yin et al., 2023; Rosay et al., 2019; de Almeida Florencio et al., 2018), traffic monitoring(Pan et al., 2021; Sun et al., 2025; Jabakumar, 2023; Zhang et al., 2024), automatic speech recognition(Malik et al., 2021; Siniscalchi et al., 2014) and various AIoT-enabled deployment scenarios(Chi et al., 2024; Fatan et al., 2016; Miryala et al., 2022; Sivapalan et al., 2022). Yet, edge devices yield $< 1\%$ of cloud servers' peak FLOPS, especially on edge devices without GPU or NPU. The dense matrix multiplication inherent to MLPs imposes a significant computational burden on resource-constrained edge devices, which severely compromises the real-time inference deadlines of edge AI applications, as Figure 1 demonstrates.

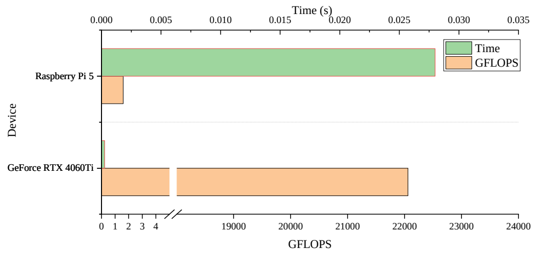

Figure 1: **Edge vs. Commercial GPU:** computational power comparison and latency of large scale matrix multiplication

Despite the pressing demand for real-time MLP inference at the edge, a general and effective solution remains absent. Existing optimization methods such as quantization and pruning primarily aim at compression; inference acceleration is a limited by-product, which typically yield $< 4\times$ speed-up(Xiao et al., 2023; Liu et al., 2025). In this paper, we introduce a simple yet effective solution: replacing the MLP with first-order Taylor expansion. Our insight is straightforward that the first-order Taylor expansion can transform an MLP, which involves multiple matrix multiplications, into a single matrix multiplication, provided that the relevant coefficients of the Taylor expansion are precomputed. Due to the nature of Taylor expansion, the approximation accuracy is contingent on the distance between the expansion point and the actual input. Thus, to confine the bulk of the input distribution to the high-probability vicinity of each expansion point, we perform K-means clustering, adopt the resulting centroids as expansion points, and precompute and cache the Taylor coefficients at each centroid. In this way, we transform the MLP to a single K-means prediction, followed by one dense matrix multiplication, dramatically speeding up inference while preserving the original prediction accuracy. Experimental results demonstrate that out method achieves **>100×** speed-up for large-scale MLPs on edge devices.

We provide theoretical complexity analysis demonstrating the superiority of our method over the native MLP, and empirically validate it on commercial edge hardware. Further experiment explored the impact of width, height, and activation choice of MLP on the approximation fidelity. Finally, we analyze the conditions under which optimal efficacy is attained.

In summary, our contributions are as follows:

1) To the best of our knowledge, we are the first to leverage approximation for MLP acceleration, offering a novel paradigm for efficient edge inference.

2) We derive a rigorous error upper bound for our method and systematically analyze how hardware characteristics influence its efficacy.

3) We conduct experiments on commercial off-the-shelf edge devices and validate the practical efficacy of our method. And experimental results demonstrate that our method achieves **>100×** speed-up for large-scale MLPs on edge devices.

2 Related Work

2.1 MLP Optimization Methods

To enable efficient MLP inference, existing studies predominantly optimize MLPs via model compression. Common compression techniques include quantization, pruning and Low-rank Factorization, etc(Dantas et al., 2024). Quantization is a method that converts high-bit floating-point parameters to low-bit integers, enabling efficient model inference(Gholami et al., 2022; Kim et al., 2023). Leveraging low-bit computation, quantization enables acceleration on general-purpose CPUs; however, the speed-up is inherently hardware-constrained and typically capped at $< 4\times$(Xiao et al., 2023; Frantar et al., 2022). Pruning accelerates inference by structurally or non-structurally eliminating unimportant weights or neurons, thereby reducing model redundancy(Vadera & Ameen, 2022). However, the sparsity introduced by pruning yields marginal acceleration, typically less than $2\times$(Hu & Yuan, 2025; Liu et al., 2025). Low-rank factorization accelerates inference by approximating the original large matrix with the product of two smaller matrices(Goyal et al., 2019; Ou et al., 2024). Yet, the actual acceleration is highly dependent on the factorization quality and hardware mapping, thus speed-up is not guaranteed.

In essence, these techniques are devised for model compression; inference acceleration is not their primary objective. Besides, our approach is orthogonal to existing methods and can be concatenated to yield simultaneously compact and highly efficient models for edge devices.

2.2 Approximate Matrix Multiplication

For acceleration-oriented inference, approximation serves as a potential viable paradigm. Approximate Matrix Multiplication (AMM) constitutes a pivotal research avenue for accelerating large-scale matrix products. The prevailing paradigm projects the operand matrices into a lower-dimensional space and subsequently performs an exact multiplication on the compressed representations(Liberty, 2013; Ghashami et al., 2016; Teng & Chu, 2019). Representative strategies include matrix sketching algorithms that deterministically(Francis & Raimond, 2022; Huang, 2019; Luo et al., 2019) or randomly construct projection matrices to curtail computational cost(Nelson & Nguyên, 2013; Dasgupta et al., 2010; Pagh, 2013; Kyrillidis et al., 2014; Sarlos, 2006). These methods only consider each matrix in isolation. And there are works that introduce variations which take into account both matrices(Francis & Raimond, 2018; Ye et al., 2016; Mroueh et al., 2016).

More recently, several works(Blalock & Guttag, 2017; 2021) have borrowed the insight of Product Quantization (PQ)(Ge et al., 2014): the vector product $A^T B$ is transformed into a sequence of table lookups and several additions. Concretely, the input vector A is partitioned into disjoint sub-vectors a_i; each a_i is assigned to its nearest centroid c_i obtained by clustering over the training data. The partial inner products $c_i^T b_i$ are precomputed and stored in a lookup table, so the online evaluation of $A^T B$ reduces to centroid indexing, table retrieval, and several additions, drastically shrinking the arithmetic complexity.

Originally devised for isolated matrix multiplications, these approaches cannot approximate a complete MLP; yet, the product-quantization philosophy inspires us to approximate the MLP directly. Instead of approximating isolated matrix products via discrete lookup tables, we approximate the entire MLP as a continuous, piecewise-linear function.

3 METHOD

To enable real-time MLP inference on edge devices, we propose an approximation-centric acceleration scheme. We first presents our method, termed T-MLP, and then provides a theoretical justification of its efficacy.

3.1 TAYLOR EXPANSION COUNTERPART

Our method approximates an MLP via first-order Taylor expansion:

$$MLP(x) \approx MLP(c_i) + \nabla MLP(c_i)^T (x - c_i). \tag{1}$$

which comprises two distinct phases: the offline phase (Steps 1–3) for precomputing $MLP(c_i)$ and $\nabla MLP(c_i)^T$ and the inference phase (Step 4) for dispatching and calculating, as illustrated in Figure 2.

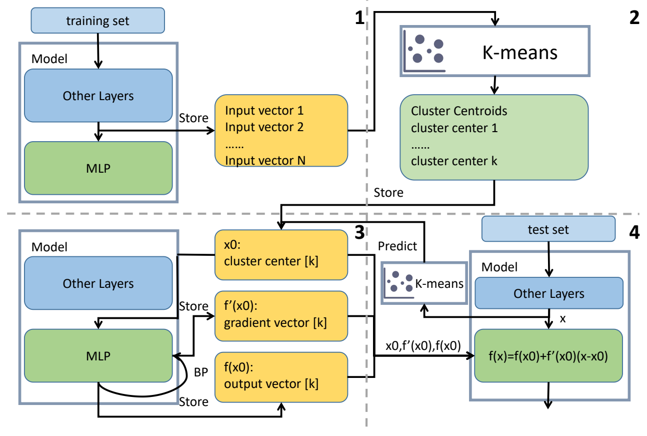

Figure 2: Flow chart of T-MLP. **Step 1:** collect the input fed to MLP. **Step 2:** cluster the input. **Step 3:** precompute and store the Taylor expansion coefficients. **Step 4:** inference with T-MLP.

During the offline phase, we first identify the Taylor expansion points and precompute the corresponding outputs and gradients. The fidelity of the first-order Taylor approximation degrades with the Euclidean distance $|x - c_i|$. To minimize this discrepancy across the entire data manifold, we apply K-means clustering on the training inputs to obtain a representative set of centroids $\{c_i\}_{i=1}^k$ and perform Taylor expansion about these centroids. To identify the centroids, we first perform the forward pass of the well trained model over the training data set and collect every input vectors fed to the MLP, which are subsequently compressed into k representative centroids by K-means. For every centroid c_i, we perform the forward pass again to obtain output as $MLP(c_i)$, and then perform back-propagation to compute the corresponding gradient $\nabla MLP(c_i)^T$.

During the inference phase, an incoming input x is dispatched to the nearest centroid c_i in the learned code-book. And the final prediction is then delivered by the first-order Taylor expansion centred at c_i.

3.2 THEORETICAL ANALYSIS

A typical MLP can be regarded as a highly intricate composite function:

$$f(x) = W_n(\sigma(\ldots\sigma(W_1(x)))), \tag{2}$$

Applying a first-order Taylor expansion to this complex composite function yields an elegant linear approximation (T-MLP):

$$f(x) \approx f(x_0) + \nabla f(x_0)^T(x - x_0), \tag{3}$$

where $f(x_0)$ and $\nabla f(x_0)$ represents the MLP's output and first-order gradient at the expansion point x_0, which can be obtained and cached offline. With T-MLP, the MLP is transformed to a single K-means prediction, followed by one dense matrix multiplication and two element-wise additions.

Considering the time complexity, a conventional MLP requires $O(N_1 \times N_2 + \cdots + N_{L-1} \times N_L)$ operations, where L represents the number of layers of MLP, and N_i represents the vector dimension. Each term denotes the time complexity of one linear layer. And the time complexity of the T-MLP is $O(N_1 \times N_L + k \times N_1)$, where k is the number of cluster centers in K-means model. Evidently, for a deep and wide MLP, provided the k is set to an appropriate magnitude, T-MLP is able to effectively reduces the time complexity.

Meanwhile, by exploiting the integral-form remainder of the Taylor expansion, we establish an upper bound on the approximation error between our proposed method and the original MLP:

Theorem 3.1 (T-MLP upper error bound)**.** *Let $f : \mathbb{R}^d \to \mathbb{R}$ be twice continuously differentiable on the line segment joining c_i and x. Then the approximation error satisfies*

$$\|f(x) - \hat{f}(x)\| \le \frac{1}{2} \sup_{z\in[c_i,x]} \|\nabla^2 f(z)\|_{\text{op}} \cdot \|x - c_i\|^2. \tag{4}$$

The detailed derivation is provided in the Appendix.

Theoretical analysis establishes that computational savings are guaranteed whenever the asymptotic cost of the Taylor expansion-based approximation falls below that of the standard MLP. In theory, a larger k yields higher approximation accuracy at the expense of diminishing speed-up; however, the practical trade-off is more nuanced, and our experiments demonstrate that k exerts only a marginal impact on the overhead of the proposed method.

4 EXPERIMENTS

In this section, to empirically validate the proposed approach. To the best of our knowledge, this work presents the first attempt to accelerate MLP inference through approximation; therefore, we adopt the original MLP as our primary baseline. We evaluate its performance on two representative edge workloads: image classification and network-intrusion detection. All experiments are conducted on a Raspberry Pi 5 (4 GB) on a single CPU core, a commodity edge device equipped with a 64-bit Arm Cortex-A76 processor without discrete GPU or NPU.

4.1 IMAGE CLASSIFICATION

Image classification is the gateway task for vision applications on edge devices. For the image-classification task, we trained the classical VGG-16(Simonyan & Zisserman, 2014) model on the CIFAR-100 dataset(Krizhevsky, 2009). The model stacks thirteen convolutional layers and terminates in a three-stage MLP classifier whose fully-connected layers are dimensioned as (512, 4096), (4096, 4096), and (4096, 100), each followed by ReLU activations. After 200 epochs of training, the model achieves 72.2 % top-1 accuracy on the CIFAR-100 test set. We replace the classifier of VGG16 with T-MLP, with the number of centroids progressively increasing from 5 to 320. The experiment results are depicted in Tables 1 and Figures 3.

Table 1: VGG 16 Experiments on Raspberry Pi 5. ACC denote the accuracy of T-MLP. T_{conv}, T_{MLP}, T_{kmeans}, $T_{expansion}$ respectively denote the latency of the convolutional layers, the original MLP, the K-means prediction, and the Taylor expansion computation. $T_{conv+MLP}$ and $T_{conv+T-MLP}$ reports the latency of original VGG16 and our proposed method.

K	Acc	MSE	T_{conv}	T_{MLP}	T_{kmeans}	$T_{expansion}$	$T_{conv+MLP}$	$T_{conv+T-MLP}$
5	72.09	156.04	0.07448	0.30363	1.05E-4	1.51E-4	0.37811	0.06878
25	72.21	60.43	0.07304	0.31335	1.17E-4	1.54E-4	0.3864	0.06950
60	72.03	28.19	0.0649	0.30377	1.45E-4	1.56E-4	0.36866	0.06636
100	72.17	13.48	0.07684	0.31489	1.68E-4	1.57E-4	0.39173	0.07061
180	72.35	11.87	0.06977	0.31583	2.20E-4	1.63E-4	0.38447	0.06626
320	72.17	10.61	0.06977	0.30252	3.29E-4	1.64E-4	0.37114	0.06599

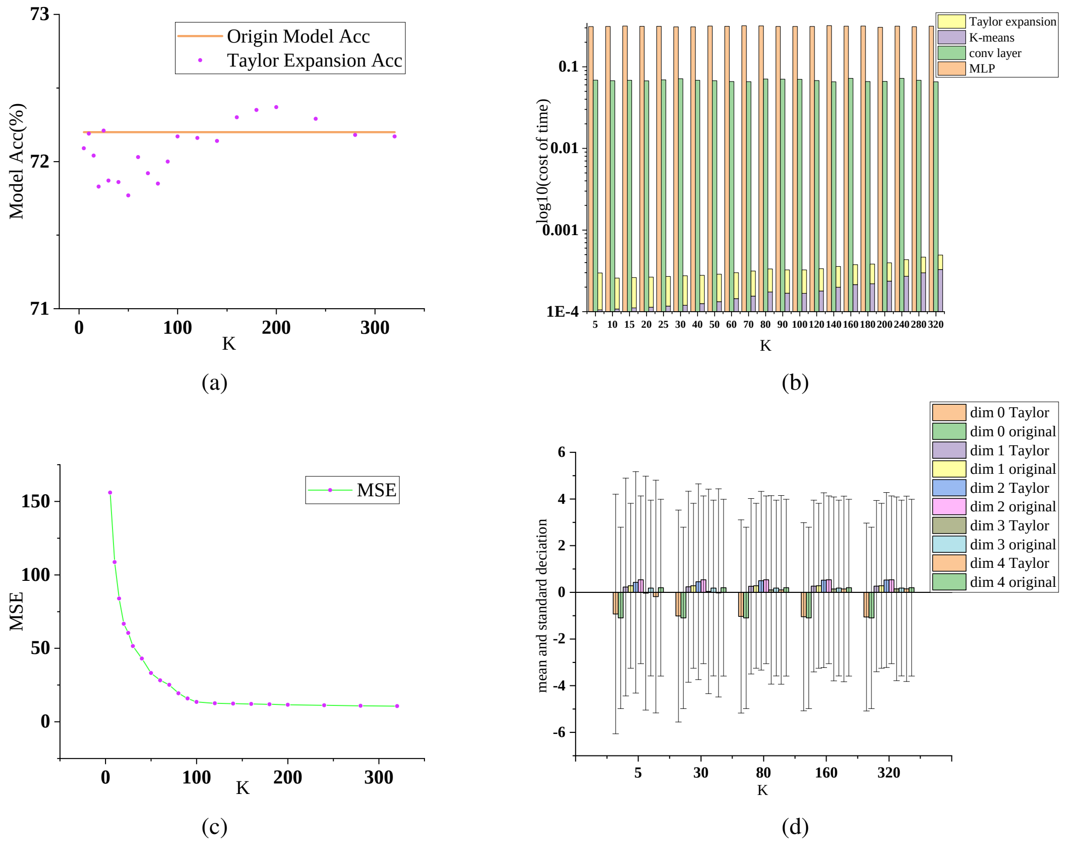

Figure 3: Experiments result of VGG-16 on Cifar-100. **(a)** : The comparison of Top-1 accuracy of original VGG-16 and its T-MLP on the Cifar-100 test set. **(b)** : The latency of the VGG-16 convolutional layers, MLP, and its T-MLP, including K-means prediction and Taylor expansion computation on Raspberry Pi 5. **(c)** : The mean square error between the 100-dimensional class-score vectors produced by the original VGG-16 model and T-MLP. **(d)** : The mean and standard deviation of the first five dimensions of the 100-dimensional output vectors generated by the original VGG-16 model and its T-MLP.

On this 100-class classification task, the T-MLP's top-1 accuracy retains the original top-1 accuracy to within 1%. And in terms of latency, far beyond our expectation, the T-MLP achieves a surprising $> 100\times$ inference acceleration. When the convolutional backbone is included, end-to-end inference is still accelerated by $6\times$. To quantify fidelity, we measured the Mean-Square Error(MSE) between the two output distributions. MSE decreases monotonically with increasing k, indicating progressively tighter approximation fidelity. Inspection of the first five dimensions of output vectors corroborates this trend: at $k = 5$ the standard deviations differ by > 1, whereas at $k = 320$ both means and variances are statistically indistinguishable.

4.2 Network Intrusion Detection

Table 2: MLP Experiments on Raspberry Pi 5. ACC denote the accuracy of T-MLP. T_{MLP}, T_{kmeans}, $T_{expansion}$ respectively denote the latency of the original MLP, the K-means prediction, and the Taylor expansion computation. And T_{T-MLP} reports the latency of our proposed method

K	Acc	MSE	T_{MLP}	T_{kmeans}	$T_{expansion}$	T_{MLP}	T_{T-MLP}
5	85.13	43.10	5.67E-4	8.19E-5	7.02E-5	5.67E-4	1.52E-4
20	96.60	6.84	5.26E-4	6.20E-5	4.90E-5	5.26E-4	1.11E-4
35	96.73	3.89	5.79E-4	6.30E-5	5.10E-5	5.79E-4	1.14E-4
50	96.97	3.09	5.28E-4	6.26E-5	4.96E-5	5.28E-4	1.12E-4
90	97.75	1.38	5.06E-4	6.57E-5	4.98E-5	5.06E-4	1.16E-4
150	98.04	0.90	5.14E-4	6.81E-5	5.06E-5	5.14E-4	1.18E-4

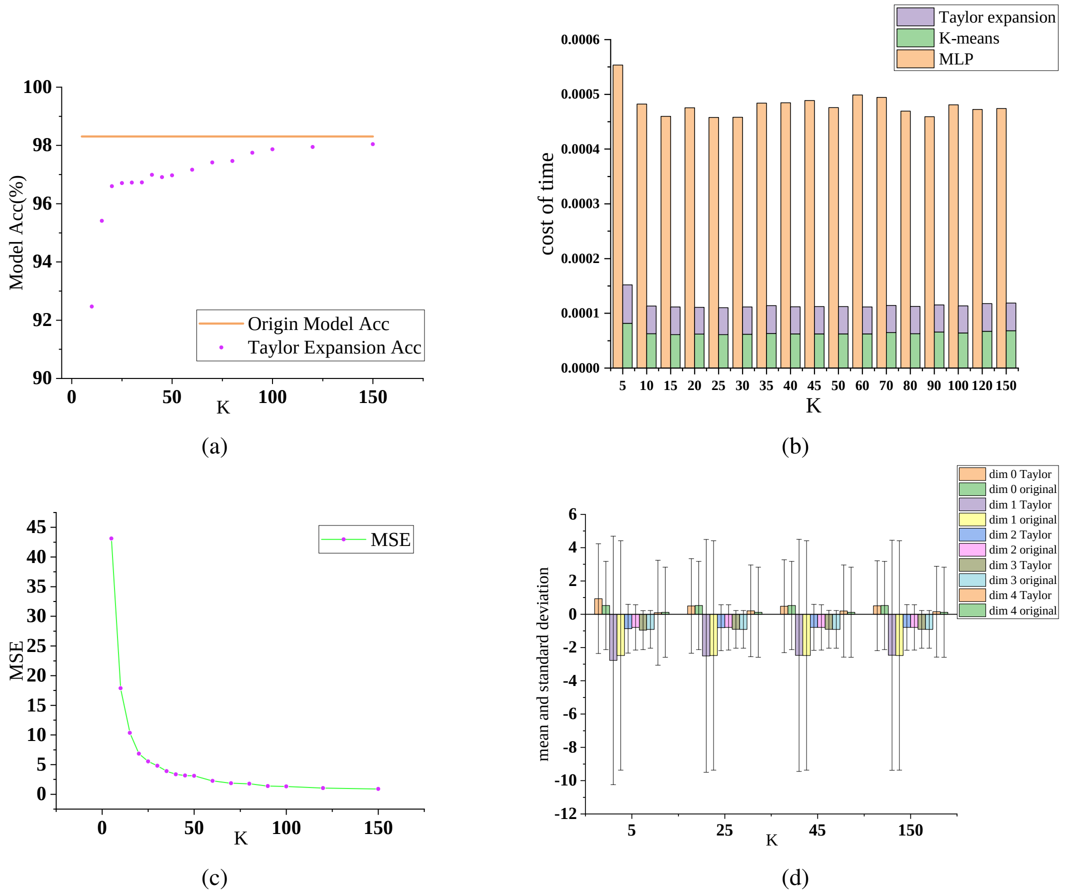

Figure 4: Experiments result of MLP on NSL-KDD. **(a)** : The comparison of Top-1 accuracy of original MLP and its T-MLP on the NSL-KDD test set. **(b)** : The latency of the MLP, and its T-MLP, including K-means prediction and Taylor expansion computation on Raspberry Pi 5. **(c)** : The mean square error between the 23-dimensional class-score vectors produced by the original MLP and its T-MLP. **(d)** : The mean and standard deviation of the first five dimensions of the 23-dimensional output vectors generated by the original MLP and its T-MLP.

To secure resource-constrained edge networks, real-time identification of anomalous traffic is essential. Network-intrusion detection is thus a critical task at the edge-side network. We evaluate our method on NSL-KDD(Tavallaee et al., 2009), a de-facto standard benchmark for intrusion-detection systems (IDS). For the network intrusion detection task, we trained a three layer MLP on the NSL-KDD dataset. The MLP layers are dimensioned as (42, 256), (256,96), and (96, 23), respectively, and we use ReLU as activation functions. The model achieves 98.31% top-1 accuracy on the NSL-KDD test set. Analogous to the preceding experiment, we replace the three-layer MLP with T-MLP, while progressively increasing the k values from 5 to 150. The experimental results are depicted in Table 2 and Figure 4.

In contrast to the previous experiment, the Taylor expansion counterpart on NSL-KDD starts with a pronounced accuracy deficit for small k, yet the gap narrows rapidly and collapses to 0.3 % when k reaches 150. In terms of latency, the T-MLP still achieves a $4\times$ inference-speedup. And the counterpart reproduces the previously observed fidelity trend: MSE versus the original MLP decreases monotonically with the increment of k, and the empirical mean and standard deviation of the first-five dimensions of output vectors converge to their original values.

4.3 Ablation Studies

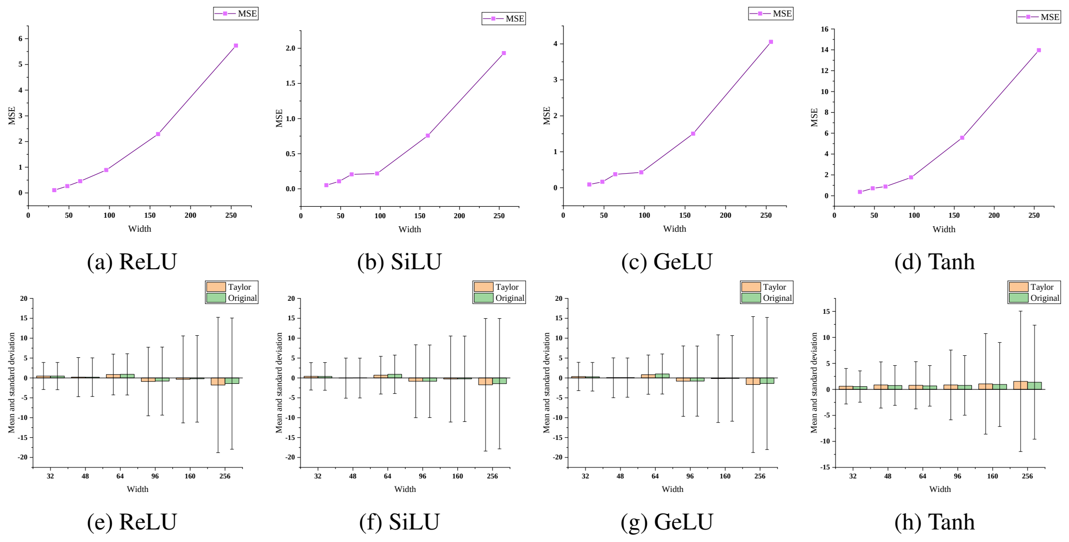

(a) ReLU (b) SiLU (c) GeLU (d) Tanh

(e) ReLU (f) SiLU (g) GeLU (h) Tanh

Figure 5: This figure shows how the model's output evolves with increasing width after the MLP is replaced by its T-MLP. **(a-d)** : how the mean-square error between the outputs of the original MLP and its T-MLP varies as the model's width increases for ReLU, SiLU, GeLU and Tanh activation functions respectively. **(e-h)** : how the mean and standard deviation between the outputs of the original MLP and its T-MLP varies as the model's width increases for ReLU, SiLU, GeLU and Tanh activation functions respectively.

To systematically investigate how the architectural complexity of MLPs influences the fidelity of their Taylor expansion counterparts, we conducted a controlled ablation study. We utilized the canonical breast cancer dataset(Wolberg & Street, 1993) to train multi-layer perceptrons (MLPs) of varying widths and heights. After randomly reserving 20 % of the instances as a held-out test set, we fitted a K-means model with k = 32 on the remaining training data.

Architecture sweeps were performed along two independent axes: width and height. In the width ablation experiment, height was held constant at 3 layers, while the hidden width increased from 32 to 256. And in height ablation experiment, width was fixed at 32 per hidden layer, while the number of hidden layers progressively increased. For every configuration we recorded three summary statistics: MSE, mean, and standard deviation between the outputs of the original MLP and its corresponding T-MLP. Additionally, we assessed the sensitivity of our approximation to the choice of activation function by repeating the above protocol under four canonical activations: ReLU, SiLU, GeLU and Tanh. The input, hidden, and output layers were dimensioned as (30, width), (width, width), and (width, 1), respectively. And all models are trained on the training set for 50 epochs. Comprehensive results are reported in Figure 5,6.

Figures 5 and 6 illustrate how the approximation capability of the T-MLP evolves with model width and height under four distinct activation functions. As the width and height of the original MLP increase, its expressive power grows accordingly, leading to a more complex and rapidly varying loss landscape. Consequently, the first-order Taylor expansion employed by T-MLP struggles to capture these fine-grained nonlinearities, and the approximation capacity consistently deteriorates regardless of the activation function used. This trend suggests that deeper and wider networks require a larger number of centroids to maintain acceptable fidelity.

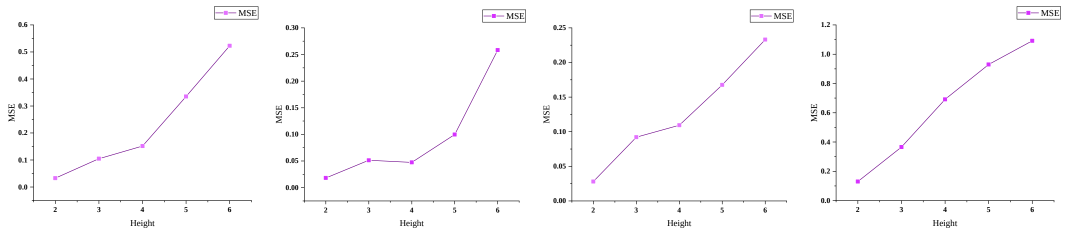

(a) ReLU (b) SiLU (c) GeLU (d) Tanh

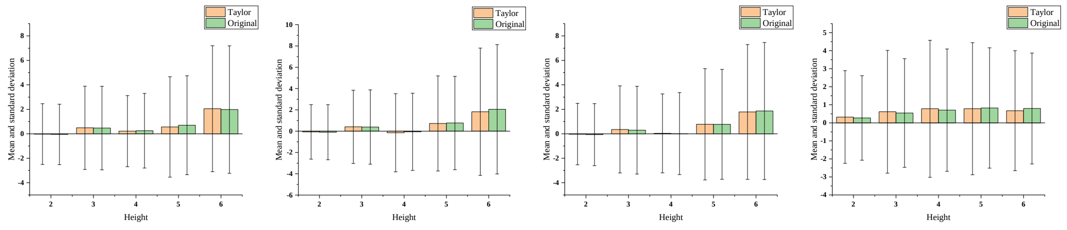

(e) ReLU (f) SiLU (g) GeLU (h) Tanh

Figure 6: This figure shows how the model's output evolves with increasing height after the MLP is replaced by its T-MLP. **(a-d)** : how the mean-square error between the outputs of the original MLP and its T-MLP varies as the model's height increases for ReLU, SiLU, GeLU and Tanh activation functions respectively. **(e-h)** : how the mean and standard deviation between the outputs of the original MLP and its T-MLP varies as the model's height increases for ReLU, SiLU, GeLU and Tanh activation functions respectively.

We also evaluate the acceleration effect of T-MLP under varying model widths and heights, as illustrated in the Figure 7. The input, hidden, and output layers were dimensioned as (512, width), (width, width), and (width, 1), and k is set to 512. As predicted by our complexity analysis, the computational gap between the original MLP and T-MLP widens with height and width increasing. At height=3 and width=512, our method already delivers $> 5\times$ speed-up. Moreover, the acceleration grows super-linearly with increasing width and height, confirming that T-MLP is especially advantageous for large-scale T-MLP.

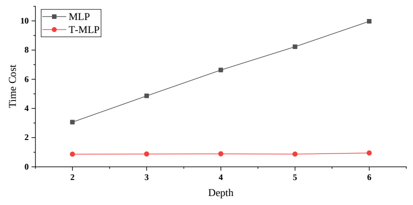

(a) Height

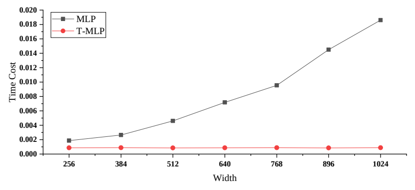

(b) Width

Figure 7: The influence of model height and width on speed-up

5 Discussions

In this section, we interpret the observed phenomena and derive the conditions under which optimal acceleration–accuracy trade-offs are achieved.

To begin with, we examine how MLP scale conditions the inference acceleration of our approach. Experiments consistently reveal a positive scaling law: speed-up grows super-linearly with model scale.This trend is first guaranteed by the reduced theoretical complexity, and is further amplified by hardware properties.

As illustrated in Figure 8, although K-means prediction initially incurs slightly higher latency than matrix multiplication at small scales, the crossover occurs as dimensionality grows, and the gap widens thereafter. This is because, despite identical asymptotic complexity, K-means distance computation outperforms matrix multiplication in practice due to reduced memory write-backs and superior SIMD utilization.

On the other hand, the experimental platform itself also matters. On contemporary CPUs, GEMM performance transitions from a compute-bound to a memory-bandwidth-bound regime once the matrix scale exceeds the threshold of cache. And as illustrated in Figure 8, the latency of matrix multiplication does not exhibit a quadratic relationship with matrix size; instead, it undergoes a step-wise increase once the scale exceeds the cache threshold. Yet this overhead is mitigated by our approach, which drastically shrinks the matrix-multiplication footprint. The Raspberry Pi 5 is equipped with a 512 KB L1 cache and a 2MB L2 cache and VGG16's classifier exceeds 60 MB, which is far beyond the cache threshold. Whereas our method confines the matrix multiplication size to the L1 cache, yielding orders-of-magnitude speed-ups.

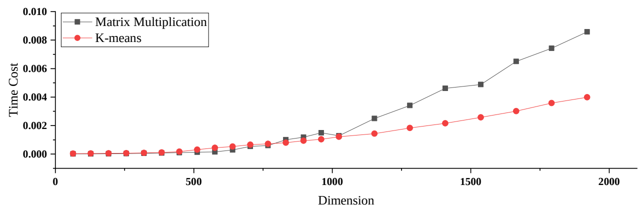

Figure 8: Time cost of different configurations of matrix multiplication $(1 \times N) \times (N \times N)$ and K-means prediction$(k = N, dim = N)$.

Next, we examine the fidelity of our approximation. The upper bound reveals that approximation fidelity hinges on the the local curvature (Hessian norm) and the distance between the actual input and its assigned centroid. The Euclidean distance between them monotonically decreases with the number of clusters k. Thus, a larger k yields a strictly tighter bound in expectation.

Empirically, the required K is strongly modulated by the data geometry. In Image Classification, VGG-16 delivers 512-D deep features that are highly coherent and clustering-friendly; consequently k = 320 already suffices to approximate the MLP. Conversely, in the Network Intrusion Detection experiment, the NSL-KDD dataset provides only 42 raw hand-crafted metrics whose scales, units, and marginal distributions are heterogeneous, thus a larger k is required. However, both theoretical complexity and empirical experiments indicate that the latency of T-MLP is less sensitive to the choice of k than to model width, validating the adoption of a larger k in practice.

In summary, our method excels when (i) the number of centroids k is sufficiently large, (ii) the MLP is of substantial scale, and (iii) the target device is memory-bandwidth-constrained.

6 Conclusion

We propose a novel approach for efficient MLP inference on edge devices by replacing the original network with its first-order Taylor expansion anchored at K-means centroids, achieving substantial latency reduction. Theoretical analysis and extensive experiments corroborate the effectiveness of the proposed method, and we further delineate the sufficient conditions for maintaining optimal performance.

In the future work, we will incorporate second- and higher-order Taylor expansions and systematically investigate the trade-offs among cluster budget k, expansion order, and inference latency.

REFERENCES

Davis Blalock and John Guttag. Multiplying matrices without multiplying. In Marina Meila and Tong Zhang (eds.), *Proceedings of the 38th International Conference on Machine Learning*, volume 139 of *Proceedings of Machine Learning Research*, pp. 992–1004. PMLR, 18–24 Jul 2021. URL `https://proceedings.mlr.press/v139/blalock21a.html`.

Davis W. Blalock and John V. Guttag. Bolt: Accelerated data mining with fast vector compression. *CoRR*, abs/1706.10283, 2017. URL `http://arxiv.org/abs/1706.10283`.

Cheng Chi, Zihang Yin, Yang Liu, and Senchun Chai. A trusted cloud–edge decision architecture based on blockchain and mlp for aiot. *IEEE Internet of Things Journal*, 11(1):201–216, 2024.

Pierre Vilar Dantas, Waldir Sabino da Silva, Lucas Carvalho Cordeiro, and Celso Barbosa Carvalho. A comprehensive review of model compression techniques in machine learning. *Applied Intelligence*, 54(22):11804–11844, September 2024. ISSN 0924-669X.

Anirban Dasgupta, Ravi Kumar, and Tamás Sarlos. A sparse johnson: Lindenstrauss transform. In *Proceedings of the Forty-Second ACM Symposium on Theory of Computing*, STOC '10, pp. 341–350, New York, NY, USA, 2010. Association for Computing Machinery. ISBN 9781450300506.

Felipe de Almeida Florencio, Edward David Moreno, Hendrik Teixeira Macedo, Ricardo JP de Britto Salgueiro, Filipe Barreto do Nascimento, and Flavio Arthur Oliveira Santos. Intrusion detection via mlp neural network using an arduino embedded system. In *2018 VIII Brazilian symposium on computing systems engineering (SBESC)*, pp. 190–195. IEEE, 2018.

Mehdi Fatan, Mohammad Reza Daliri, and Alireza Mohammad Shahri. Underwater cable detection in the images using edge classification based on texture information. *Measurement*, 91:309–317, 2016.

Deena P. Francis and Kumudha Raimond. An improvement of the parameterized frequent directions algorithm. *Data Min. Knowl. Discov.*, 32(2):453–482, March 2018. ISSN 1384-5810.

Deena P. Francis and Kumudha Raimond. A practical streaming approximate matrix multiplication algorithm. *Journal of King Saud University - Computer and Information Sciences*, 34(1):1455–1465, 2022. ISSN 1319-1578.

Elias Frantar, Saleh Ashkboos, Torsten Hoefler, and Dan Alistarh. Gptq: Accurate post-training quantization for generative pre-trained transformers. *arXiv preprint arXiv:2210.17323*, 2022.

Tiezheng Ge, Kaiming He, Qifa Ke, and Jian Sun. Optimized product quantization. *IEEE Transactions on Pattern Analysis and Machine Intelligence*, 36(4):744–755, 2014.

Mina Ghashami, Edo Liberty, Jeff M. Phillips, and David P. Woodruff. Frequent directions: Simple and deterministic matrix sketching. *SIAM J. Comput.*, 45(5):1762–1792, January 2016. ISSN 0097-5397.

Amir Gholami, Sehoon Kim, Zhen Dong, Zhewei Yao, Michael W Mahoney, and Kurt Keutzer. A survey of quantization methods for efficient neural network inference. In *Low-power computer vision*, pp. 291–326. Chapman and Hall/CRC, 2022.

Saurabh Goyal, Anamitra Roy Choudhury, and Vivek Sharma. Compression of deep neural networks by combining pruning and low rank decomposition. In *2019 IEEE International Parallel and Distributed Processing Symposium Workshops (IPDPSW)*, pp. 952–958, 2019.

Andrew G Howard, Menglong Zhu, Bo Chen, Dmitry Kalenichenko, Weijun Wang, Tobias Weyand, Marco Andreetto, and Hartwig Adam. Mobilenets: Efficient convolutional neural networks for mobile vision applications. *arXiv preprint arXiv:1704.04861*, 2017.

Hanyu Hu and Xiaoming Yuan. Spap: Structured pruning via alternating optimization and penalty methods. *arXiv preprint arXiv:2505.03373*, 2025.

Zengfeng Huang. Near optimal frequent directions for sketching dense and sparse matrices. *J. Mach. Learn. Res.*, 20(1):2018–2040, January 2019. ISSN 1532-4435.

A Kingsly Jabakumar. Edge-enabled smart traffic management system: An iot implementation for urban mobility. *Research journal of computer systems and engineering*, 4(2):160–173, 2023.

Sehoon Kim, Coleman Hooper, Thanakul Wattanawong, Minwoo Kang, Ruohan Yan, Hasan Genc, Grace Dinh, Qijing Huang, Kurt Keutzer, Michael W Mahoney, et al. Full stack optimization of transformer inference: a survey. *arXiv preprint arXiv:2302.14017*, 2023.

Alex Krizhevsky. Learning multiple layers of features from tiny images. 2009. URL `https://api.semanticscholar.org/CorpusID:18268744`.

Anastasios Kyrillidis, Michail Vlachos, and Anastasios Zouzias. Approximate matrix multiplication with application to linear embeddings. In *2014 IEEE International Symposium on Information Theory*, pp. 2182–2186, 2014.

Edo Liberty. Simple and deterministic matrix sketching. In *Proceedings of the 19th ACM SIGKDD International Conference on Knowledge Discovery and Data Mining*, KDD '13, pp. 581–588. Association for Computing Machinery, 2013. ISBN 9781450321747.

Ji Lin, Wei-Ming Chen, Yujun Lin, Chuang Gan, Song Han, et al. Mcunet: Tiny deep learning on iot devices. *Advances in neural information processing systems*, 33:11711–11722, 2020.

Ji Lin, Wei-Ming Chen, Han Cai, Chuang Gan, and Song Han. Memory-efficient patch-based inference for tiny deep learning. *Advances in Neural Information Processing Systems*, 34:2346–2358, 2021.

Shuqi Liu, Bowei He, Han Wu, and Linqi Song. Optishear: Towards efficient and adaptive pruning of large language models via evolutionary optimization. *arXiv e-prints*, pp. arXiv–2502, 2025.

Luo Luo, Cheng Chen, Zhihua Zhang, Wu-Jun Li, and Tong Zhang. Robust frequent directions with application in online learning. *Journal of Machine Learning Research*, 20(45):1–41, 2019. URL `http://jmlr.org/papers/v20/17-773.html`.

Mishaim Malik, Muhammad Kamran Malik, Khawar Mehmood, and Imran Makhdoom. Automatic speech recognition: a survey. *Multimedia Tools and Applications*, 80(6):9411–9457, 2021.

Sandeep Miryala, Md Adnan Zaman, Sandeep Mittal, Yihui Ren, Grzegorz Deptuch, Gabriella Carini, Sioan Zohar, Shinjae Yoo, Jack Fried, Jin Huang, et al. Peak prediction using multi layer perceptron (mlp) for edge computing asics targeting scientific applications. In *2022 23rd International Symposium on Quality Electronic Design (ISQED)*, pp. 1–6. IEEE, 2022.

Youssef Mroueh, Etienne Marcheret, and Vaibhava Goel. Co-occuring directions sketching for approximate matrix multiply. *CoRR*, abs/1610.07686, 2016. URL `http://arxiv.org/abs/1610.07686`.

Jelani Nelson and Huy L. Nguyên. Osnap: Faster numerical linear algebra algorithms via sparser subspace embeddings. In *2013 IEEE 54th Annual Symposium on Foundations of Computer Science*, pp. 117–126, 2013.

Xinwei Ou, Zhangxin Chen, Ce Zhu, and Yipeng Liu. Low rank optimization for efficient deep learning: Making a balance between compact architecture and fast training. *Journal of Systems Engineering and Electronics*, 35(3):509–531, 2024.

Rasmus Pagh. Compressed matrix multiplication. *ACM Trans. Comput. Theory*, 5(3), August 2013. ISSN 1942-3454.

Shengli Pan, Peng Li, Changsheng Yi, Deze Zeng, Ying-Chang Liang, and Guangmin Hu. Edge intelligence empowered urban traffic monitoring: A network tomography perspective. *IEEE Transactions on Intelligent Transportation Systems*, 22(4):2198–2211, 2021.

Marius-Constantin Popescu, Valentina Balas, Liliana Perescu-Popescu, and Nikos Mastorakis. Multilayer perceptron and neural networks. *WSEAS Transactions on Circuits and Systems*, 8, 07 2009.

Arnaud Rosay, Florent Carlier, and Pascal Leroux. Mlp4nids: An efficient mlp-based network intrusion detection for cicids2017 dataset. In *International Conference on Machine Learning for Networking*, pp. 240–254. Springer, 2019.

Mark Sandler, Andrew Howard, Menglong Zhu, Andrey Zhmoginov, and Liang-Chieh Chen. Mobilenetv2: Inverted residuals and linear bottlenecks. In *Proceedings of the IEEE conference on computer vision and pattern recognition*, pp. 4510–4520, 2018.

Tamas Sarlos. Improved approximation algorithms for large matrices via random projections. In *2006 47th Annual IEEE Symposium on Foundations of Computer Science (FOCS'06)*, pp. 143–152, 2006.

Karen Simonyan and Andrew Zisserman. Very deep convolutional networks for large-scale image recognition. *Computer Science*, 2014.

Sabato Marco Siniscalchi, Torbjørn Svendsen, and Chin-Hui Lee. An artificial neural network approach to automatic speech processing. *Neurocomputing*, 140:326–338, 2014.

Gawsalyan Sivapalan, Koushik Kumar Nundy, Soumyabrata Dev, Barry Cardiff, and Deepu John. Annet: A lightweight neural network for ecg anomaly detection in iot edge sensors. *IEEE Transactions on Biomedical Circuits and Systems*, 16(1):24–35, 2022.

Jingru Sun, Chendingying Lu, Yichuang Sun, Hongbo Jiang, and Zhu Xiao. Online transfer learning with mlp-assisted graph convolution network for traffic flow forecasting: A solution for edge intelligent devices. *Frontiers of Information Technology & Electronic Engineering*, 2025.

Mahbod Tavallaee, Ebrahim Bagheri, Wei Lu, and Ali A. Ghorbani. A detailed analysis of the kdd cup 99 data set. In *2009 IEEE Symposium on Computational Intelligence for Security and Defense Applications*, pp. 1–6, 2009.

Dan Teng and Delin Chu. A fast frequent directions algorithm for low rank approximation. *IEEE Transactions on Pattern Analysis and Machine Intelligence*, 41(6):1279–1293, 2019.

Sunil Vadera and Salem Ameen. Methods for pruning deep neural networks. *IEEE Access*, 10: 63280–63300, 2022.

Mangasarian Olvi Street Nick Wolberg, William and W. Street. Breast Cancer Wisconsin (Diagnostic). UCI Machine Learning Repository, 1993.

Guangxuan Xiao, Ji Lin, Mickael Seznec, Hao Wu, Julien Demouth, and Song Han. Smoothquant: Accurate and efficient post-training quantization for large language models. In *International conference on machine learning*, pp. 38087–38099. PMLR, 2023.

Qiaomin Ye, Luo Luo, and Zhihua Zhang. Frequent direction algorithms for approximate matrix multiplication with applications in cca. In *Proceedings of the Twenty-Fifth International Joint Conference on Artificial Intelligence*, IJCAI'16, pp. 2301–2307. AAAI Press, 2016. ISBN 9781577357704.

Yuhua Yin, Julian Jang-Jaccard, Wen Xu, Amardeep Singh, Jinting Zhu, Fariza Sabrina, and Jin Kwak. Igrf-rfe: a hybrid feature selection method for mlp-based network intrusion detection on unsw-nb15 dataset. *Journal of Big data*, 10(1):15, 2023.

Junfeng Zhang, Cheng Xie, Hongming Cai, Weiming Shen, and Rui Yang. Knowledge distillation-based spatio-temporal mlp model for real-time traffic flow prediction. *IEEE Transactions on Intelligent Transportation Systems*, 2024.

A Appendix

In this section, we derive an upper bound on the approximation error for the vector-valued function $f : R^d \rightarrow R^m$ by means of the integral remainder.

Assume that $z_t = c_i + t(x - c_i), t \in [0, 1]$ denote the line segment between x and c_i, and function f is twice differentiable along the line segment. The first order Taylor expansion is:

$$f(x) = f(c_i) + \nabla f(c_i)^T (x - c_i). \tag{5}$$

And the integral remainder is:

$$f(x) - \hat{f}(x) = \int_0^1 (1-t)\nabla^2 f(z_t)[x - c_i, x - c_i]dt. \tag{6}$$

The Euclidean norm of the difference between the original value and its Taylor-expansion approximation is:

$$||f(x) - \hat{f}(x)|| \leq \int_0^1 (1-t)\nabla^2 f(z_t)[x - c_i, x - c_i]dt. \tag{7}$$

Since

$$||\nabla^2 f(z_t)[x - c_i, x - c_i]|| \leq sup_{||u||=1} ||\nabla^2 f(z_t)[u, u]|| \cdot ||x - c_i||^2 \tag{8}$$

Factor out the distance term and perform integration.

$$||f(x) - \hat{f}(x)|| \leq ||x - c_i||^2 \int_0^1 (1-t)\nabla^2 f(z_t)_{op} dt. \tag{9}$$

Extract the supremum of the Hessian norm over the line segment.

$$H^{(i)}_{max}(x) := sup_{\in [c_i, x]} ||\nabla^2 f(z)||_{op} \tag{10}$$

$$\int_0^1 (1-t)||\nabla^2 f(z_t)_{op}||dt \leq H^{(i)}_{max}(x) \int_0^1 (1-t)dt = \frac{1}{2} H^{(i)}_{max}(x) \tag{11}$$

Then we obtain the final upper bound.

$$||f(x) - \hat{f}(x)|| \leq \frac{1}{2} sup_{z \in [c_i, x]} ||\nabla^2 f(z)||_{op} \cdot ||x - c_i||^2 \tag{12}$$